

# InP/AlGaInAs Microring Laser and Its Application in All-optical XOR Gate

Sheng Xie

School of Electronic Information Engineer  
Tianjin University  
Tianjin, China  
e-mail: xie\_sheng06@tju.edu.cn

Zhiming Chen

Library of Hebei North University  
Zhangjiakou, China

Meiling Li

School of Electronic Information Engineer  
Tianjin University  
Tianjin, China

Jing Guo

School of Electronic Information Engineer  
Tianjin University  
Tianjin, China

**Abstract**—Due to the versatile functions and the potential ability of monolithic integration, semiconductor ring laser (SRL) has received increasing attention recently in the application of all-optical logic unit. In this paper, InP/AlGaInAs multiple quantum well (MQW) ring lasers with different cavity structures were designed and fabricated using the optimized process parameters. The measurement results shown that the fabricated microring lasers have a wide bistability operation regime, and are suitable for the all-optical logic gate and the optical random storage memory. Based on the optical bistability and the injection locking of ring laser, Boolean function  $\bar{A} \cdot B$  was demonstrated by using one of the monolithic integrated ring lasers, and an all-optical XOR gate can be obtained by two completely symmetrical SRLs integrated on one chip.

**Keywords**- semiconductor ring laser; microcavity; optical bistability; logic gate; multiple quantum well

## I. INTRODUCTION

With the rapid development of optical fiber transmission technology, ultra high-speed signal processing capacity at the switching nodes in optical communication systems is required<sup>[1]</sup>. Unfortunately, due to the speed limitation of electronic devices, the conventional electro-optical conversion and ultra-fast electronics scheme has been accepted more and more challenges. To realize the next generation ultra high-speed communication networks, a potential solution is to substitute the electronic devices with all-optical switching and signal processing units. Compared to the conventional electro-optical conversion scheme, the all-optical solution has the advantages of high-speed and low power consumption.

To make the all-optical network come true, it is necessary that entire components used in the optical networks should be all-optical elements. All-optical logic gate as an essential element is indispensable to construct the future all-optical networks. Up to now, various all-optical gates have been proposed and implemented based on different methods and elements. Initially, all-optical logic gates based on semiconductor optical amplifier (SOA) properties were reported<sup>[2-4]</sup>. However, due to the limitation of power consumption, operation speed and

structure size, SOA has being substituted gradually by the novel device and concept. Recently, all-optical reconfigurable AND, NOR, and XOR gates for nonreturn-to-zero (NRZ) format signal are realized in the highly nonlinear fiber (HNLF)<sup>[5]</sup> and the nonlinear optical loop mirror (NOLM)<sup>[6]</sup>. And all-optical logic gates have been also demonstrated by means of the photonic crystal<sup>[7]</sup> and microring resonators<sup>[8]</sup>.

Presently, semiconductor ring laser (SRL) has attracted more and more attention because of its compact device structure, versatile functions, and compatibility. Up to now, SRL has been used for tunable laser<sup>[9]</sup>, wavelength-routing switch<sup>[10]</sup>, wavelength converter<sup>[11]</sup>, and optical memory<sup>[12]</sup>. Due to the robust optical bistability<sup>[13]</sup> and injection locking effect<sup>[14]</sup>, the potential ability of SRL for all-optical logic gates has been experimentally verified<sup>[15]</sup>. More recently, a novel monolithic all-optical toggle flip-flop (TFF) with two complementary output was demonstrated based on the intrinsic bistability of SRL and the saturable absorption effect occurred in the reverse-biased input waveguide, and a recorded bit-rate of 500Mb/s for all-optical TFFs was achieved<sup>[16]</sup>. Comparing with the other methods and elements to carry out the all-optical logic gate, the logic units based on SRL have the advantages of compact device structure, low switching energy, high output extinction ratio, and stable operation<sup>[15]</sup>. As a result, SRL is considered as a potential candidate for constructing large-scale photonic integrated circuits.

In this paper, InP/AlGaInAs MQW ring lasers with different cavity structures were designed and fabricated. The experimental results indicated that the fabricated microring lasers have excellent optical bistability. Based on the robust bistable properties and injection locking effect of SRL, an all-optical NOR gate was demonstrated by using one of the monolithic integrated microring lasers. Depending on the expression of XOR function, the all-optical XOR gate can be carried out by two completely symmetrical SRLs.

## II. FABRICATION AND CHARACTERIZATION OF SRL

A commercially available InP/AlGaInAs multiple quantum well (MQW) epitaxial wafer is adopted. The key structural parameters are described in Table I. In this paper,

different structure devices with circular and racetrack shaped resonator were designed and realized<sup>[17]</sup>. To minimize back-reflection, the bus waveguide has a 10° tilt angle with respect to the cleaved facets.

TABLE I. PARAMETERS OF INP/ALGAINAS EPITAXIAL WAFER

Layer	Material	Thickness /nm	Refractive index
Cap layer	P-Ga <sub>0.47</sub> In <sub>0.53</sub> As	200	3.64
Upper clapping	P-InP	1600	3.17
GRIN	i-Al <sub>0.42-0.34</sub> GaIn <sub>0.53</sub> As	100	3.25
Barrier	i-Al <sub>0.22</sub> Ga <sub>0.29</sub> In <sub>0.49</sub> As	10	3.38
Quantum well	i-Al <sub>0.07</sub> Ga <sub>0.22</sub> In <sub>0.71</sub> As	5×10	3.55
Barrier	i-Al <sub>0.22</sub> Ga <sub>0.29</sub> In <sub>0.49</sub> As	5×10	3.38
GRIN	i-Al <sub>0.42-0.34</sub> GaIn <sub>0.53</sub> As	100	3.25
Lower cladding	N-InP	2000	3.17

Firstly, the ring laser patterns were created on PMMA with electron-beam lithography. Using magnetically enhanced reactive ion etching (MERIE) system, the PMMA mask was transferred to an underlying SiO<sub>2</sub> layer to provide a hard mask. The InP/AlGaInAs epitaxial wafer was etched by an Oxford Plasmalab inductively coupled plasma (ICP) machine with chlorine, methane and argon process gases<sup>[18]</sup>. The flow rates as well as the other etching parameters had been optimized. The etch profiles of the parallel waveguide directional coupler was shown in Fig. 1. As seen in this figure, a smooth etched surface and a vertical ridge profile were obtained, making our optimized process well adapted to the realization of shallow etched microring laser.

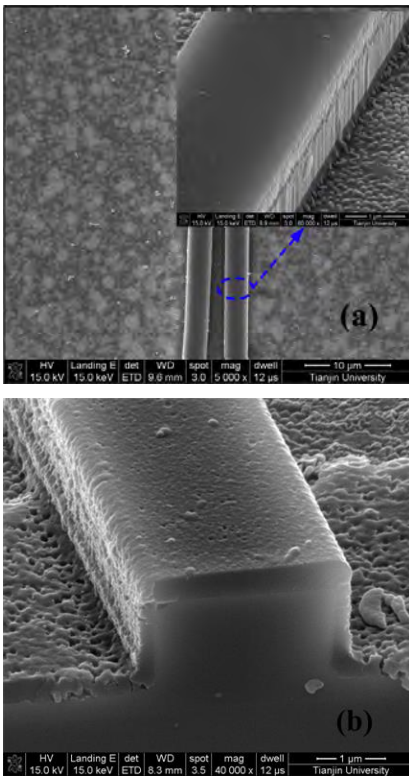


Figure 1. SEM Micrograph of the directional coupler etched by ICP

Then, an insulating layer, which was also used for surface planarization, was spun on the wafer after the

complete removal of the residual SiO<sub>2</sub> mask. The p- and n-type ohmic contacts were prepared by sputtering Ti/Au metal stack and AuGeNi alloy, respectively. To measure the intensity of counter propagating lasing modes simultaneously, integrated photodetectors (PDs) were fabricated on both ends of the bus waveguide. It's important to note that the PDs can also work as SOA when they are positively biased. The photograph of fabricated ring laser is shown in Fig. 2. The two devices (SRL1 and SRL2) given in Fig. 2 have completely symmetrical structure, and the resonator is formed with two semi-circular sections with 298 μm radius and two 113 μm long bus waveguide.

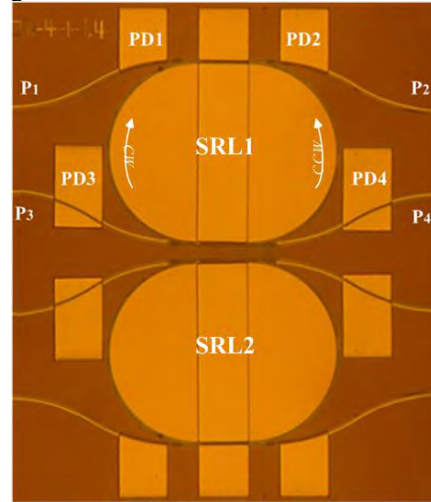


Figure 2. Photograph of InP/AlGaInAs MQW ring laser with racetrack shaped cavity

To characterize the electrical and optical properties of fabricated ring lasers, the photocurrent of lasers was fed to Keithley 4200, and the operation temperature of the tested devices was controlled by a thermal control circuit. A typical current-voltage (I-V) characteristic of the fabricated microring laser diodes was shown in Fig. 3. As seen in the figure, the forward turn-on voltage and reverse breakdown voltage were respectively 0.4V and 10.6V@1μA, which is similar to that of the conventional semiconductor laser diode with Fabry-Perot cavity<sup>[19]</sup>.

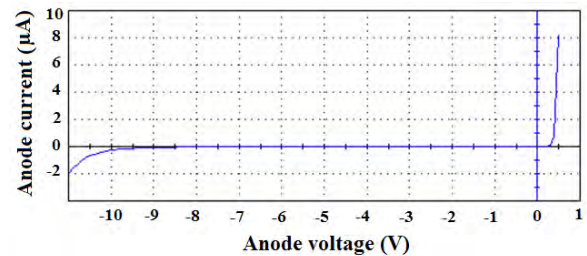


Figure 3. Typical I-V characteristics of InP/AlGaInAs laser diode

The optical bistability between the clockwise (CW) and counterclockwise (CCW) modes was shown in Fig. 4. As we can see, the tested ring laser (SRL1) has a threshold current of 65 mA, and directly entered into the unidirectional bistability regimes once the driving current exceeded the threshold current. Thus, the driving current and power consumption of bistability operation are reduced greatly, and the fabricated devices are very

suitable to the all-optical logic gate and random storage memory.

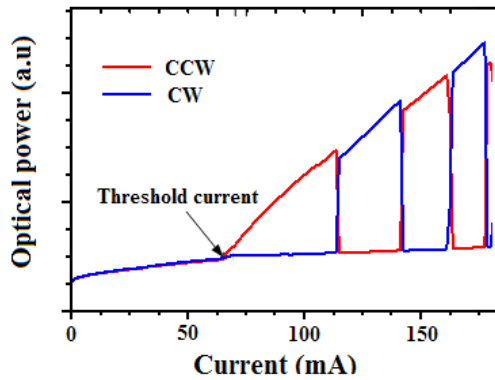


Figure 4. P-I characteristic of the InP/AlGaInAs MQW ring laser

### III. ALL-OPTICAL XOR GATE

Based on the optical bistability and injection locking effect of SRL, the all-optical logic gate had been implemented by one of the fabricated SRLs. However, due to the limitation of experimental setup and design deviation, the all-optical NOR gate was demonstrated only by using one of the monolithic integrated SRLs (SRL1) in this paper. The simplified schematic of measurement was shown in Fig. 5. The return-to-zero (RZ) format input signal A is generated by a pulse pattern generator and modulates the light from tunable laser (TL1) by Mach-Zehnder modulator (MZM1). To boost the signal power, an erbium-doped fiber amplifier (EDFA1) is inserted in the channel of signal A, and then attenuated by a variable optical attenuator (Att.1) to adjust the power level of signal A injected into the device under test (DUT) via port 1 (P1). The RZ input signal B is generated using the same process as signal A excepted an additional optical delay line (ODL), and injected into the ring laser via port 2 (P2). The ODL is used to match the delay between the two signals A and B. Depending on the signal power, CW or CCW mode of SRL1 was locked, and the output current signal from port 3 (P3) was fed to a oscilloscope (OSC).

In the following experiment, SRL1 was biased at 130 mA in the stable unidirectional operation regime. During the measurement, no biases were applied on the integrated PD1, PD2, and PD4, while the PD3 was biased at -0.5 V, which converts the output light power into photocurrent signal.

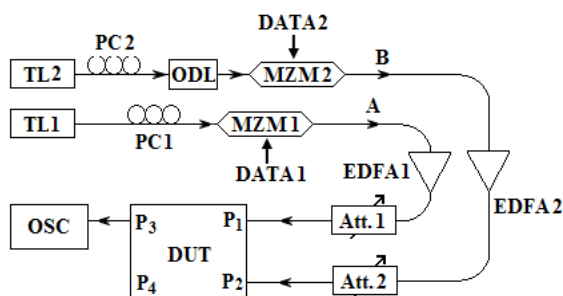


Figure 5. Simplified schematic of measurement.

The power level of signals A and B on both sides of SRL1 were adjust by Att.1 and Att.2 such that signal A has a higher power for logic level “1” than that of signal B, while its “0” power is lower than the “1” power of signal B, but higher than the “0” power of signal B, that is,  $I_{A>1B}>0_A>0_B$ . Whatever CW or CCW mode was present in SRL1, the CW mode was activated and injection locked when the signal A has a high power “1”. The CW mode of SRL1 was held when the two signals had a logic level “0”. Only when the signal A has a low power “0”, and the signal B has a high power “1” simultaneously, the CW mode was switched to the CCW mode. As a result, SRL1 was alternatively injection locked by signals A and B depending on the power levels. Thus, Boolean function  $\bar{A} \cdot B$  can be obtained from SRL1.

Fig. 6 shows the patterns of two input signals and the output results of all-optical  $\bar{A} \cdot B$  gate. Where Fig. 6(a) and (b) represents the bit pattern of signals A and B, respectively. The final output pattern shown in Fig. 6(c) denotes a code stream of “10010001001000” that is exactly the  $\bar{A} \cdot B$  function between input signals A and B.

Similarly, if we swap the power level of two signals A and B, and inject them into the other monolithic integrated SRL (SRL2) that has a completely symmetrical structure, Boolean function  $A \cdot \bar{B}$  can also be achieved. Therefore, the XOR function can be obtained by a linear superposition of  $\bar{A} \cdot B$  and  $A \cdot \bar{B}$  through a 3dB power combiner.

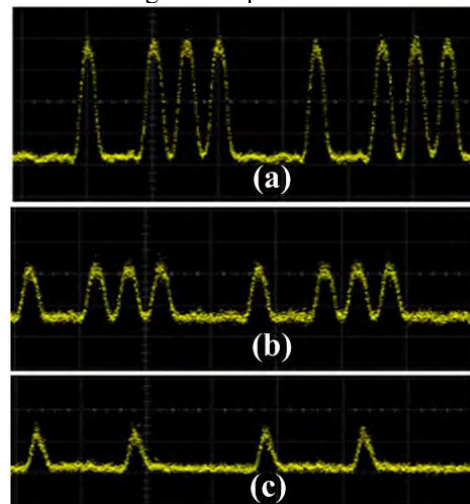


Figure 6. Experimental results of all-optical  $\bar{A} \cdot B$  gate. (a) pattern of signal A, (b) pattern of signal B, (c) pattern of all-optical  $\bar{A} \cdot B$  function

### IV. CONCLUSION

InP/AlGaInAs MQW microring lasers with circular and racetrack shaped structure were designed and fabricated. The experimental results shown that smooth etched surfaces and vertical ridge profiles can be obtained using the optimized etching process. The racetrack shaped laser with a circumference of 2 097  $\mu\text{m}$  has a threshold current of 65 mA, and the device directly entered into the unidirectional bistability regimes once the driving current exceeded the threshold current.

Based on the optical bistability and injection locking effect of SRL, Boolean function  $\bar{A} \cdot B$  was demonstrated by using one of the fabricated microring lasers, and an all-optical XOR gate can be obtained by two completely

symmetrical SRLs. The theoretical and experimental results indicate that SRL is a multi-purpose photonic unit<sup>[20]</sup> that can be used to realize most of the functions required by the photonic integrated circuits.

#### ACKNOWLEDGMENT

The work was supported by the National Natural Science Foundation of China under Grant 61106052.

#### REFERENCES

- [1] H. C. H. Mulvad, E. Palushani, H. Hu, H. Ji, M. Galili, A. T. Clausen, P. Jeppesen, and L. K. Oxenløwe, "Recent Advances in ultra-high-speed optical signal processing," *Proc. Eur Conf Opt Commun (ECOC 12)*, IEEE Press, Sep. 2012, pp. Tu.1.A.5-1-2, doi: 10.1364/ECEOC.2012.Tu.1.A.5.
- [2] A. Hamie, A. Sharaiha, M. Guegan, B. Pucel, "All-optical logic NOR gate using two-cascaded semiconductor optical amplifiers," *IEEE Photon. Technol. Lett.*, vol.14, pp.1439-1441, Oct. 2002, doi: 10.1109/LPT.2002.802426.
- [3] J. Y. Kim, S. K. Han, and L. Seok, "All-optical multiple logic gates with XOR, NOR, OR and NAND functions using parallel SOA-MZI structures: Theory and experiment", *IEEE J. Photon. Technol.*, vol.24, pp.3392-3399, Sep. 2006, doi: 10.1109/JLT.2006.880593.
- [4] S. Singh, and Lovkesh, "Ultrahigh Speed Optical Signal Processing Logic Based on an SOA-MZI," *IEEE J. Sel. Top. Quantum Electron.*, vol.18, pp. 970-977, Mar. 2012, doi:10.1109/JSTQE.2011.2155623.
- [5] L. Li, J. Wu, J. Qiu, B. Wu, K. Xu, X. Hong, Y. Li, and J. Lin, "Reconfigurable all-optical logic gate using four-wave mixing (FWM) in HNLF for NRZ-PolSK signal," *Opt. Commun.*, vol.283, pp. 3608-3612, Oct. 2010, doi:10.1016/j.optcom.2010.05.028.
- [6] W. Wang, J. Yu, J. Luo, B. Han, J. Guo, J. Wang, Y. Liu, and E. Yang, "40Gb/s reconfigurable all-optical logic gate based on nonlinear optical loop mirror," *Acta Optica Sinica*, vol.32, pp. 0506003, May 2012, doi: 10.3788/AOS201232.0506003.
- [7] Y. Fu, X. Hu, and Q. Gong, "Silicon photonic crystal all-optical logic gate" *Phys. Lett. A*, vol.377, pp. 329-333, Jan. 2013, doi: 10.1016/j.physleta.2012.11.034.
- [8] A. Fushimi, and T. Tanabe, "All-optical logic gate operating with single wavelength," *Opt. Express*, vol.22, pp.4466-4479, Feb. 2014, doi: 10.1364/OE.22.004466.
- [9] S. Kim, Y. T. Byun, D. G. Kim, N. Dagli, and Y C Chung, "Widely tunable coupled ring reflector laser diode consisting of square ring resonators," *J. Opt. Soc. Korea*, vol.14, pp. 38-41, Mar. 2010, doi: 10.3807/JOSK.2010.14.1.038.
- [10] T. Segawa, S. Matsuo, T. Kakisuka, Y. Shibata, and T. Sato, "Monolithically integrated wavelength-routing switch using tunable wavelength converters with double-ring-resonator tunable Lasers," *IEICE Trans. Electron.*, vol.E94-C, pp. 1439-1446, Sep. 2011, doi: 10.1587/transele.E94.C.1439.
- [11] C. W. Tee, K. A. Williams, R. V. Pentyl, I. H. White, "Vertically coupled microring laser array for dual-wavelength generation," *Proc. Conf. Lasers Electro-Opt. (CLEO 07)*, IEEE Press, May 2007, pp. CThB6-1-2, doi: 10.1109/CLEO.2007.4452687.
- [12] M. T. Hill, H. J. S. Dorren, T. de Vries, J. M. Leijtens, and J. H. den Besten, "A fast low-power optical memory based on coupled micro-ring laser". *Nature*, vol.432, pp. 206-208, Nov. 2004, doi: 10.1038/nature03045.
- [13] G. Mezösi, M. J. Syrain, S. Fürst, Z. Wang, S Yu, and M. Sorel, "Unidirectional bistability in AlGaInAs microring and microdisk semiconductor lasers," *IEEE Photon. Technol. Lett.*, vol.21, pp.88-90, Jan. 2009, doi: 10.1109/LPT.2008.2008660.
- [14] G. Yuan, Z. Wang, B. Li, M. I. Memon, and S. Yu, "Theoretical and experimental studies on bistability in semiconductor ring lasers with two optical injections," *IEEE J. Sel. Top. Quantum Electron.*, vol.14, pp.903-910, May 2008, doi: 10.1109/JSTQE.2008.918058.
- [15] B. Li, M. I. Memon, G. Mezosi, Z. Wang, M. Sorel, and S Yu, "All-optical digital logic gates using bistable semiconductor ring lasers," *J Opt. Commun.*, vol.30, pp.190-194, Dec. 2009.
- [16] A. Trita, G. Mezosi, M. Sorel, G. Giuliani, "All-optical toggle flip-flop based on monolithic semiconductor ring laser". *IEEE Photon. Technol. Lett.* vol.26, pp. 96-99, Jan. 2014, doi: 10.1109/LPT.2013.2289976.
- [17] S. Xie, J. Guo, K. Guan, L. Mao, W. Guo, L. Qi, and X Li, "Design and realization of InP/AlGaInAs multiple quantum well ring laser," *Trans. Tianjin Univ.*, vol.20, pp.402-406, Dec. 2014, doi: 10.1007/s12209-014-2387-3.
- [18] S. Xie, Z. Chen, X. Yu, S. Zhang, X. Li, Y. Chen, W. Guo, L. Qi, L. Mao, and J. Yu, "Effect of ICP etching on InP-based multiple quantum wells microring lasers," *Proc. IEEE Int. Conf. Electron Devices Solid-State Circuits (EDSSC 11)*, IEEE Press, Nov. 2011, pp.1-2, doi: 10.1109/EDSSC.2011.6117681.
- [19] C Z Sun, J Wang, Q W Zhou, B Xiong, and Y Luo, "Room temperature dry etching of InP-based semiconductors for optoelectronic device fabrication using inductively coupled plasma," *Proc Int. Conf. Indium Phosphide and Relat. Mater.* IEEE Press, May 2007, pp.229-232, doi: 10.1109/ICIPRM.2007.381165.
- [20] S. Yu, "All-optical functions based on semiconductor ring lasers," *Chin. Opt. Lett.*, vol.8, pp.918-923, Sep. 2010, doi: 10.3788/COL.20100809.0918